Original

Etoposide-Induced Cellular Senescence Suppresses Autophagy in Human Keratinocytes

Mizuki Yoshida[1), Saki Takahashi[2), Nanako Tsuchimochi[3), Hanako Ishii[4), Toru Naito[1) and Jun Ohno[5)

[1) *Section of Geriatric Dentistry, Department of General Dentistry, Fukuoka Dental College, Fukuoka, Japan*
[2) *Section of Orthodontics, Department of Oral Growth and Development, Fukuoka Dental College, Fukuoka, Japan*
[3) *Section of Periodontology, Department of Odontology, Fukuoka Dental College, Fukuoka, Japan*
[4) *Section of Pediatric Dentistry, Department of Oral Growth and Development, Fukuoka Dental College, Fukuoka, Japan*
[5) *Oral Medicine Research Center, Fukuoka Dental College, Fukuoka, Japan*
(Accepted for publication, January 17, 2023)

Abstract: Autophagy and senescence play important roles in cellular homeostasis. However, it remains unknown whether autophagy positively or negatively affects cellular senescence. We cultured human keratinocytes (HaCaT) with or without etoposide (ETO) treatment to examine whether autophagy mediates induction of DNA damage response (DDR)-related cellular senescence. DDR-related cellular senescence was observed in 5.0-μM ETO-treated cells through increased expression of γH2AX, p53 binding protein1 (53BP1), and senescence-associated β-galactosidase (SA-β-Gal), whereas no senescent changes were observed in 1.0-μM ETO-treated cells. Senescent cells also showed increased expression of activated ataxia–telangiectasia mutated (ATM) signaling pathway-related factor, such as pATM, pp53, and p21. The 5.0-μM ETO-treated senescent cells showed downregulated expression of LC3 and Beclin-1, but expression of Rubicon, which is a negative regulator of autophagy, was upregulated even though no senescent-induced cells (1.0-μM treated cells) revealed increased expression of LC3 and Beclin-1. The 1.0-μM ETO-treated cells pretreated with N-acetylcysteine (NAC) showed increased expression of senescent markers and p21 as well as Rubicon. This study revealed that Rubicon-regulated autophagy mediates ETO-induced DDR-related cellular senescence through the activation of the ATM/p53/p21 signaling pathway. Impaired autophagy due to Rubicon overexpression accelerates induction of DDR-related cellular senescence.

Key words: Senescence, Autophagy, Rubicon, DNA damage response

Introduction

Cellular senescence is the process from embryonic development to aging. Several types of normal and tumor cells undergo cellular senescence after exposure to H_2O_2, radiation, or DNA-damaging agents[1-3]. DNA damage may lead to genomic instabilities, which is one of the key factors that induce cellular senescence[4]. DNA damage response (DDR) occurs to maintain cellular homeostasis when DNA is damaged. Furthermore, DDR seems to play an essential role in the outcome of senescence, called DDR-related cellular senescence, by disfavoring the apoptosis response[5].

Senescent cells cannot divide even if stimulated by mitogens. However, they remain metabolically and synthetically active but show characteristic changes in morphology such as an enlarged and flattened cell shape and increased granularity[6]. The most widely used assay for senescence is the histochemical and cytochemical detection of β-galactosidase activity at a pH of 6.0, which is known as senescence-associated β-galactosidase (SA-β-Gal). This activity is based on the increased lysosomal content of senescent cells, which enables the detection of lysosomal β-Gal at a suboptimal pH (pH 6.0)[7, 8]. Other canonical senescence markers comprise the common mediators of DDR-related senescence, including ataxia–telangiectasia mutated (ATM), p53, and p21, which are members of the DDR-activated ATM signaling pathway[6]. Foci of heterochromatin is also a feature of senescent cells induced by DDR and are detected by γH2AX and p53 binding protein 1 (53BP1)[9, 10].

Macroautophagy (autophagy) is an evolutionarily conserved intracellular degradation process wherein cytosolic materials, including damaged organelles and toxic protein aggregates, are sequestered in specialized double membrane-bound autophagosomes[11, 12]. By guiding the degradation of a wide range of targets, autophagy maintains cellular homeostasis and allows adaptation to stress; dysregulation of autophagy has been implicated in many human diseases, including cancer, neurodegeneration, and metabolic disorders[13, 14]. Autophagy and senescence share several common characteristics, suggesting that these processes maintain cellular homeostasis and could serve similar ends in the cell[13, 15]. However, it remains unknown whether autophagy positively or negatively affects cellular senescence. Some groups have suggested that accelerated autophagy may induce cellular senescence[16-18], whereas others proposed an association between autophagy impairment and the induction of senescence[19, 20].

Etoposide (ETO), a DNA-damaging agent, is frequently used as adjuvant chemotherapy for a variety of human malignant tumors. ETO is a topoisomerase II inhibitor that induces DNA double-strand breaks (DSBs), resulting in the induction of DDR[21] and subsequent cellular senescence[22]. This study aimed to elucidate whether autophagy mediates the induction of DDR-related cellular senescence in ETO-treated human keratinocytes (HaCaT cells) and whether autophagy impairment can accelerate cellular senescence.

Correspondence to: Dr. Jun Ohno, 2-15-1 Tamura, Sawara-ku, Fukuoka, Fukuoka 8140193, Japan; Tel: +81928010411 (Ext 1684); Fax: +81928014909; E-mail: johno@college.fdcnet.ac.jp

Materials and Methods

Reagents and antibodies

Dulbecco's modified Eagle's medium (DMEM) was purchased from Fujifilm WakoPure Chemical Co., (Osaka, Japan). Fetal bovine serum (FBS) was purchased from HyClone Laboratories Inc. (South Logan, UT, USA). N-acetylcysteine (NAC) and Hoechst 33324 nucleic acid stain were purchased from Sigma-Aldrich Corporation (St. Louis, MO, USA). SpiDER-γGal Kit was obtained from Dojindo (Kumamoto, Japan). Precision Plus Protein Western C Standard, 4%–20% and 12% Mini-PROTEAN® TGX™ Precast Gels, and Trans-Blot Transfer Packs were obtained from Bio-Rad Laboratories (Hercules, CA, USA). Sinal-Fire Plus ECL Reagent was purchased from Cell Signaling Technology (Danvers, MA, USA). Anti-LC3, anti-Beclin-1, and anti-Rubicon were purchased from MBL (Tokyo, Japan). Anti-ATM, pATM (Ser 1981), anti-p53, anti-pp53 (Ser33), and anti-p21Waf1/Cip1(p21) were purchased from Cell Signaling Technology (Danvers, MA, USA). Anti-γH2AX were obtained from Dojindo. Anti-β-actin (ACTB) and horseradish peroxidase-conjugated anti-mouse and anti-rabbit secondary antibodies were obtained from Bio-Rad Laboratories. Anti-mouse or anti-rabbit IgG (H+L) secondary antibody-Alexa Fluor Plus 568 was obtained from Thermo Fisher Scientific (Waltham, MA, USA).

Cell culture

HaCaT cells were maintained in DMEM supplemented with 10% (v/v) FBS and 1× anti-anti solution at 37ºC in a humidified incubator with 5% CO_2. For ETO stimulation, HaCaT cells at approximately 80% confluence were exposed to ETO at different concentrations (1.0, 5.0, 10, and 25 μM) for 24 h. Other cells were pretreated with NAC, which is an autophagy inhibito[23, 24], before treatment with ETO.

Cell viability test

To determine cell viability against ETO stimulation, HaCaT cells treated or untreated with ETO for 24 h were washed with phosphate-buffered saline (PBS), harvested from the dishes via trypsinization, resuspended in PBS, and diluted in 0.4% trypan blue solution in a 1:1 ratio. The percentage of viable cells was calculated using a Countess Automated Cell Counter (Invitrogen) following the manufacturer's instructions.

Senescence-associated β-galactosidase (SA-β-Gal) staining

SA-β-Gal staining of HaCaT cells was performed using a Cellular Senescence Detection Kit-SPiDER-γGal (Dojindo) according to the manufacturer's instructions. Using the WinROOF (MITANI Corp., Tokyo, Japan) image analysis software, positive and negative cells were automatically counted, and the percentage (%) of positive cells was calculated.

Immunocytochemical analysis

Cultured HaCaT cells were placed on glass slides and fixed in cold methanol. The cells were incubated with primary antibodies (γHA2X, phosphorylated ATM [pATM], phosphorylated p53 [pp53], p21, LC3, Beclin-1, and Rubicon, 1:100) at 4ºC overnight. After washing with PBS, the cells were incubated with anti-rabbit or anti-mouse IgG conjugated with Alexa Fluor 568 at room temperature for 45 min. To visualize nuclei, cells were counterstained with Hoechst 33342. The stained cells were mounted with ProLong Gold Antifade Mountant and viewed under a light microscope (Keyence Corporation of America, Elmwood Park, NJ, USA). Using the WinROOF image analysis software, positive and negative cells or nuclei were automatically counted, and the percentage

(%) of positive cells or nuclei was calculated.

Western blot analysis

HaCaT cells were lysed in a cell lysis buffer containing 1x protease/phosphatase inhibitor cocktail. Protein concentrations were measured with the Pierce BCA Protein Assay Kit. Equal amounts (15 μg) of protein along with a protein marker were separated on Mini-PROTEAN TGX Precast Gels for 30 min at 200 V. The Trans-Blot Turbo Transfer System (Bio-Rad Laboratories) was used to transfer the separated proteins to a polyvinylidene fluoride membrane. Western blots were processed using iBind Western System (Life Technologies, Carlsbad, CA, USA) with primary antibodies (× 1,000) and goat anti-mouse or anti-rabbit IgG (H+L)-HRP conjugate (× 1,000) as secondary antibodies. ACTB antibody (× 1,500: VMA00048, Bio-Rad Laboratories, Hercules, CA, USA) was used as a loading control. An enhanced chemiluminescence system (SignalFire Plus ECL Reagent; Cell Signaling Technology) was used to develop the protein bands. The protein levels were quantified by densitometry using an ImageQuant LAS 4000 bimolecular imager (GE Healthcare, Uppsala, Sweden). Band densities were presented as fold-increases of the expression levels of primary antibodies (normalized to ACTB) and compared with the results of control. Quantification results were shown below the corresponding blots. The densitometry data were from a representative of three independent experiments.

Statistical analysis

Statistical analyses were performed using EZR (Saitama Medical Center, Jichi Medical University, Saitama, Japan), which is a graphical user interface for R (The R Foundation for Statistical Computing, Vienna, Austria). Analyses were performed using one-way analysis of variance with Bonferroni's multiple comparisons test or Student's t-test to determine statistical differences among the samples. Data are presented as mean ± standard deviation (SD). and a p-value < 0.05 was considered statistically significant.

Results

ETO treatment elicited DNA damage in HaCaT cells

ETO is a potent inducer of DSBs in DNA[25]. We first examined the effects of ETO on the viability of HaCaT cells. Cell viability was inhibited by ETO (0–25 μM) in a dose-dependent manner. Trypan blue dye exclusion showed no significant differences between doses up to 5.0 μM ETO when compared with the control (Fig. 1A).

Meanwhile, cell viability was significantly decreased in cells treated with 10 and 25 μM of ETO. From these results, we selected concentrations of 1.0 and 5.0 μM ETO for further experiments.

Papanicolaou (Pap) staining was applied to elucidate the morphological changes in the nuclei of cells treated with ETO. Cells stained with Pap were polygonal with high nuclear–to–cytoplasm ratios and indistinct cell borders. Additionally, they had round to oval nuclei. Cells without ETO treatment showed fine chromatin in nuclei (Fig. 1B). Meanwhile, in cells treated with ETO, nuclear chromatin became coarse and clumped. Although some cells treated with 1.0 μM of ETO showed nuclear chromatin clumping, marked chromatin clumping was observed in most cells treated with 5.0 μM of ETO. These results indicate that chromatin clumping implies the occurrence of DSB-related DNA damage in cells treated with ETO (Fig. 1C).

We examined the immunocytochemical detection of γH2AX and 53BP1, known as biomarkers of DDR, in cells treated with 1.0 and 5.0 μM of ETO to elucidate ETO-induced cellular changes. Immunocytochemical analysis revealed that both γH2AX and 53BP1 were expressed

in nuclei as foci formation in 1.0- and 5.0-μM ETO-treated cells. The percentages of γH2AX-positive cells were significantly different between the 5.0-μM ETO-treated cells (89.2% ± 2.9%), control cells (2.8% ± 0.9%; $p < 0.01$), and 1.0-μM ETO-treated cells (53.4% ± 5.6%; $p < 0.01$) (Fig. 1D). Similarly, the percentages of 53 BP1-positive cells were significantly greater in 5.0-μM ETO-treated cells (88.7% ± 4.0%) than in control cells (10.4% ± 2.2%; $p < 0.01$) and in 1.0-μM ETO-treated

cells (74.2% ± 6.2%; $p < 0.05$) (Fig. 1D). As DNA damage was evaluated by γH2AX and 53BP1 foci formation, we counted the number of foci per cell with or without ETO treatment. The average number of foci per cell was greater in 5.0-μM ETO-treated cells (γH2AX, 15.3 ± 4.6/53BP1, 14.6 ± 5.6) than in control (γH2AX, 0.3 ± 0.4; $p < 0.01$/53BP1, 2 ± 1.3; $p < 0.01$) and in 1.0-μM ETO-treated cells (γH2AX, 5.2 ± 1.5; $p < 0.01$/53BP1,9.3 ± 3.9; $p < 0.01$) (Fig. 1D). Based on the staining intensi-
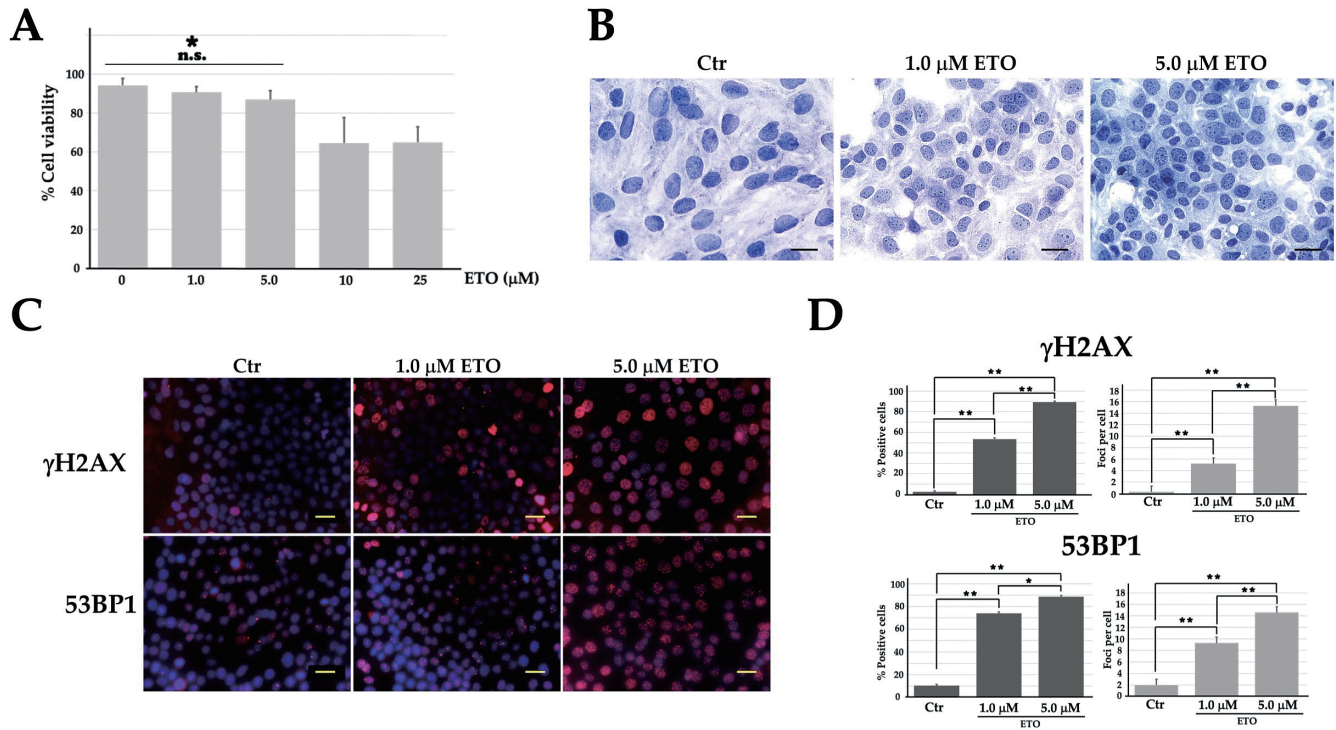

Figure 1. Induction of DNA damage response in ETO-treated cells. (A) Cell viability was determined using trypan blue exclusion. The graph shows the viability of the cells exposed to different concentrations (0, 1, 5, 10, or 25 μM) of ETO for 24 h. Results are presented as a percentage of viable cells. Data represent mean values ± SD of three independent experiments. n.s., not significant. (B) Nuclear changes were examined in human keratinocytes with or without ETO treatment using Papanicolaou staining. Scale bars represent 20 μm. (C) Immunofluorescence images of γH2AX and 53BP1 staining (red). Nuclei were counterstained with Hoechst 33342 (blue). Scale bars represent 20 μm. (D) Semiquantification of the percentage of positive cells or the number of nuclear foci that were stained with γH2AX or 53BP1 using WinROOF image analysis software. Data represent the mean ± SD of three independent experiments. *$P < 0.05$, ** $P < 0.01$. Ctr, control; ETO, etoposide; 53BP1, p53 binding protein1.
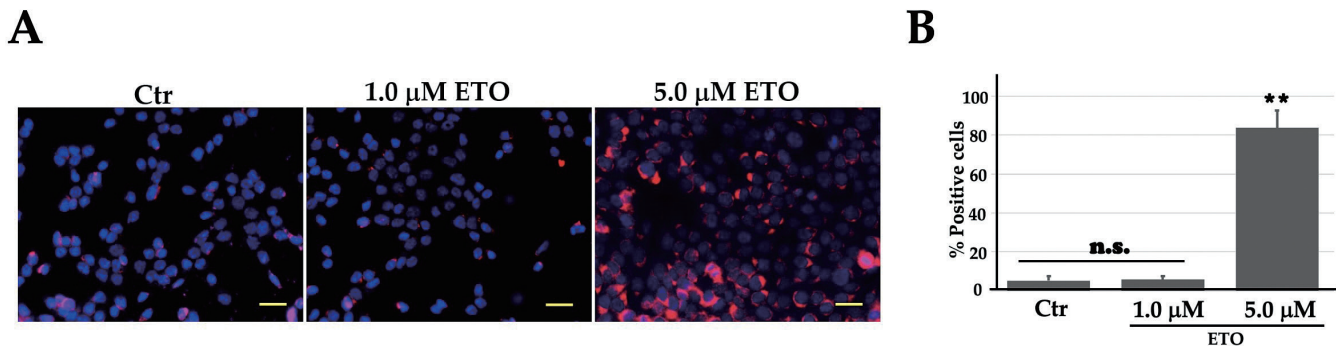

Figure 2. ETO-induced cellular senescence in human keratinocytes. (A) Fluorescence images of SA-β-Gal staining (red) using the SPiDER-βGal Kit. Nuclei were counterstained with Hoechst33324 (blue) in cells treated with 1.0 and 5.0 μM ETO. Scale bar represents 20 μm. (B) Semiquantification of the percentage of positive cells that were stained with SA-β-Gal using WinROOF image analysis software. Data represent the mean ± SD of three independent experiments. n.s., not significant. ** $P < 0.01$. Ctr, control; ETO, etoposide.

ty of γH2AX and 53BP1, the cellular changes seen with treatment with 1.0 μM ETO imply a mild phase of DDR. These findings provide evidence that both γH2AX and 53BP1 can form nuclear foci in response to ETO-induced DNA DSBs. The increased number of foci in 5.0-μM ETO-treated cells indicate that the degree of DDR is more severe than that in 1.0-μM ETO-treated cells.

Induction of cellular senescence in HaCaT cells exposed to 5.0 μM of ETO

Exposure of cells to ETO can induce cellular senescence[22, 26, 27]. To elucidate whether ETO treatment can induce cellular senescence in Ha-CaT cells, we examined SA-β-Gal, which is known as a biomarker of cellular senescence[7, 8], in cells with or without ETO treatment. Fluorescence analysis (Fig. 2A) revealed an increase in the percentages of SA-β-Gal-positive cells in 5.0-μM ETO-treated cells (5.3% ± 2.3% [control] and 5.8% ± 1.8% [1.0-μM ETO-treated cells] vs. 83.7% ± 8.9% [5.0-μM ETO-treated cells]; $p < 0.01$) (Fig. 2B). Treatment with 5.0 μM of ETO can induce cellular senescence, whereas treatment with 1.0 μM of ETO neither resulted in decreased cell viability nor the induction of cellular senescence. These findings suggest that severe DDR induced by ETO can result in cellular senescence.

ETO-induced cellular senescence is mediated by activation of the ATM pathway

Recent studies reported that ATM activation is one of the key regulators of DDR as well as promotes cellular senescence and inhibits apoptosis[28, 29]. Detection of pATM, pp53, and p21 expression was examined by immunocytochemical and WB assays. Perinuclear expression of pATM was noted in cells treated with ETO (Fig. 3A). The percentages of pATM-positive cells were significantly different between the 5.0-μM ETO-treated cells (90.0% ± 7.4%), controls (20.8% ± 2.4%; $p < 0.01$), and 1.0-μM ETO-treated cells (47.6% ± 4.2%, $p < 0.01$) (Fig. 3B). WB analysis showed that the expression levels of pATM were upregulated in 5.0-μM ETO-treated cells as compared to those in controls and in 1.0-μM ETO-treated cells (Fig. 3C). Furthermore, we examined changes in the expression levels of downstream signaling of ATM, such as pp53 and p21. In pp53 and p21 staining, the positive reaction was localized in the nuclei of cells treated with 1.0 and 5.0 μM of ETO (Fig. 3A). The percentage of pp53-positive cells was significantly higher in 5.0-μM ETO-treated cells (84.7% ± 10.0%) than in controls (2.9% ± 1.7%; $p < 0.01$) and in 1.0-μM ETO-treated cells (14.3 ± 3.3%; $p < 0.01$) (Fig. 3C). In p21 staining, the percentage of p21-positive cells was the highest in 5.0-μM ETO-treated cells (91.1% ± 7.9%) than in controls (2.1% ± 0.9; $p < 0.01$) and in 1.0-μM ETO-treated cells (9.7% ± 3.5%; $p < 0.01$) (Fig. 3B). The results of WB analysis showed that the expression levels of both pp53 and p21 were remarkably increased in 5.0-μM ETO-treated cells as compared to the control and in 1.0-μM ETO-treated cells (Fig. 3C). These results revealed that senescence-induced 5.0-μM ETO-treated cells showed increased expression of pATM, pp53, and p21. As those factors mediate DDR, this suggests that treatment with 5.0 μM of ETO induces DDR-related cellular senescence in HaCaT cells.

Induction of DDR-related cellular senescence suppresses autophagy in ETO-treated senescent cells

To elucidate whether autophagy can regulate the induction of cellular senescence, we examined the expression of positive and negative
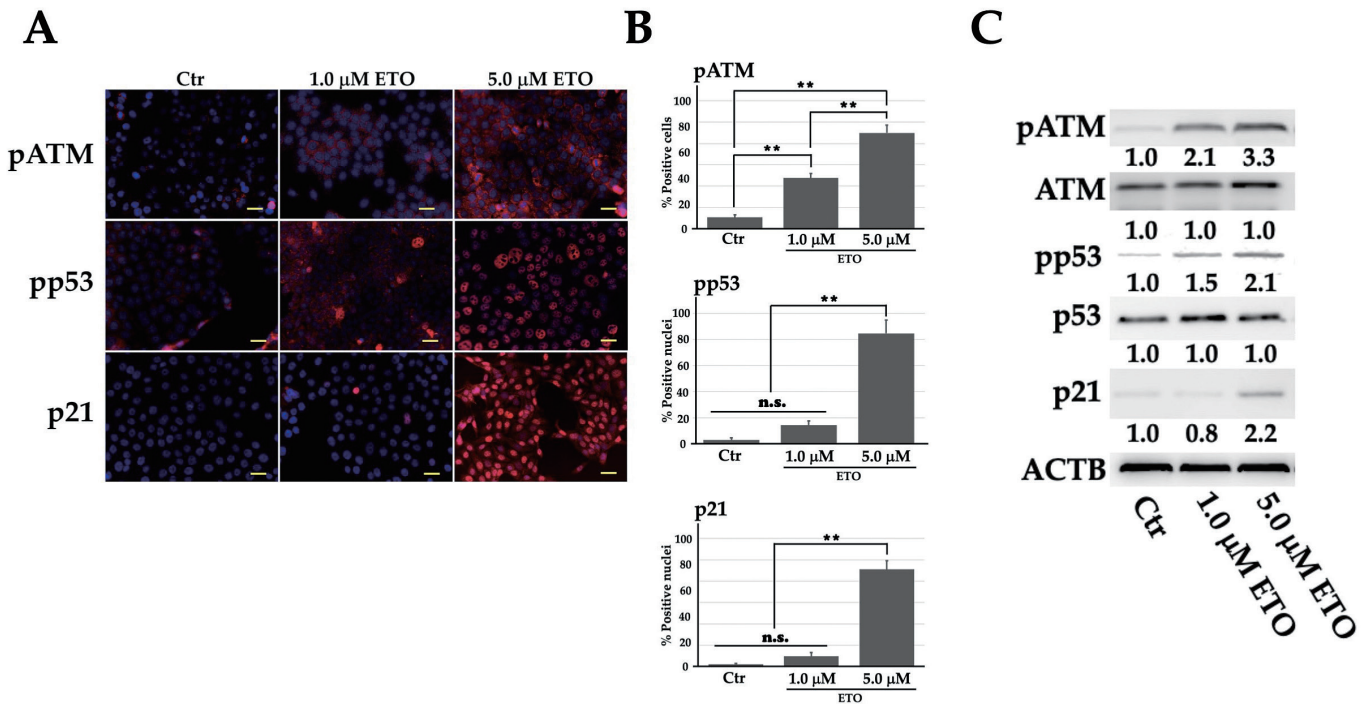

Figure 3. Activated ATM pathway in ETO-induced cells. (A) Immunofluorescence images of pATM, pp53, and p21 staining (red) in human keratinocytes treated with 1.0 and 5.0 μM of ETO. Nuclei were counterstained with Hoechst 33342 (blue). Scale bars represent 20 μm. (B) Semi-quantification of the percentage of positive cells or nuclei that were stained with pATM, pp53, and p21 using WinROOF image analysis software. Data represent the mean ± SD of three independent experiments. n.s., not significant. ** $P < 0.01$. (C) Western blot analysis of pATM, ATM, pp53, p53, p21, and ACTB in human keratinocytes treated with 1.0 and 5.0 μM of ETO. Ctr, control; ETO, etoposide; ATM, ataxia–telangiectasia mutated; pATM, phosphorylated ATM; pp53, phosphorylated p53; ACTB, β-actin.
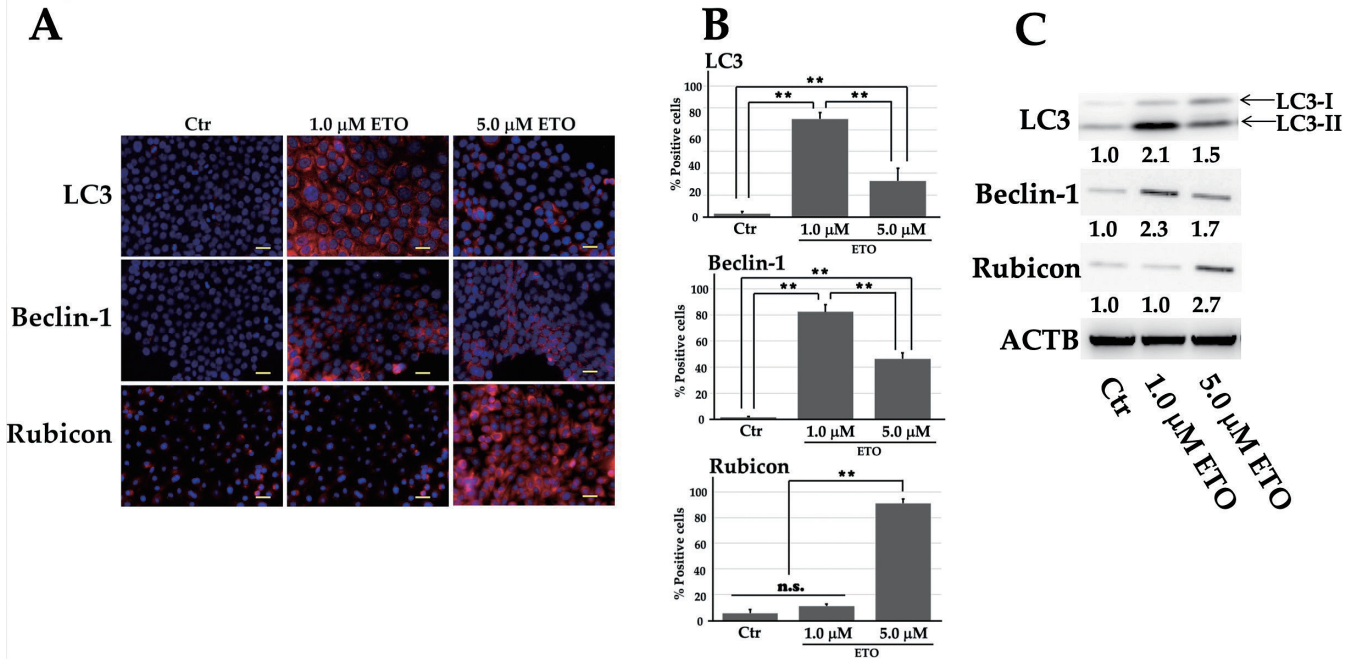
Figure 4. Suppression of autophagy in DNA damage response-related cellular senescence. (A) Immunofluorescence images of LC3, Beclin-1, and Rubicon staining (red) in human keratinocytes treated with 1.0 and 5.0 μM of ETO. Nuclei were counterstained with Hoechst 33342 (blue). Scale bars represent 20μm. (B) Semiquantification of the percentage of positive cells or nuclei that were stained with LC3, Beclin-1, and Rubicon using WinROOF image analysis software. Data represent the mean ± SD of three independent experiments. n.s., not significant. ** *P* < 0.01. (C) Western blot analysis of LC3, Beclin-1, Rubicon, and ACTB in human keratinocytes treated with 1.0 and 5.0 μM of ETO. Ctr, control; ETO, etoposide; ACTB, β-actin.
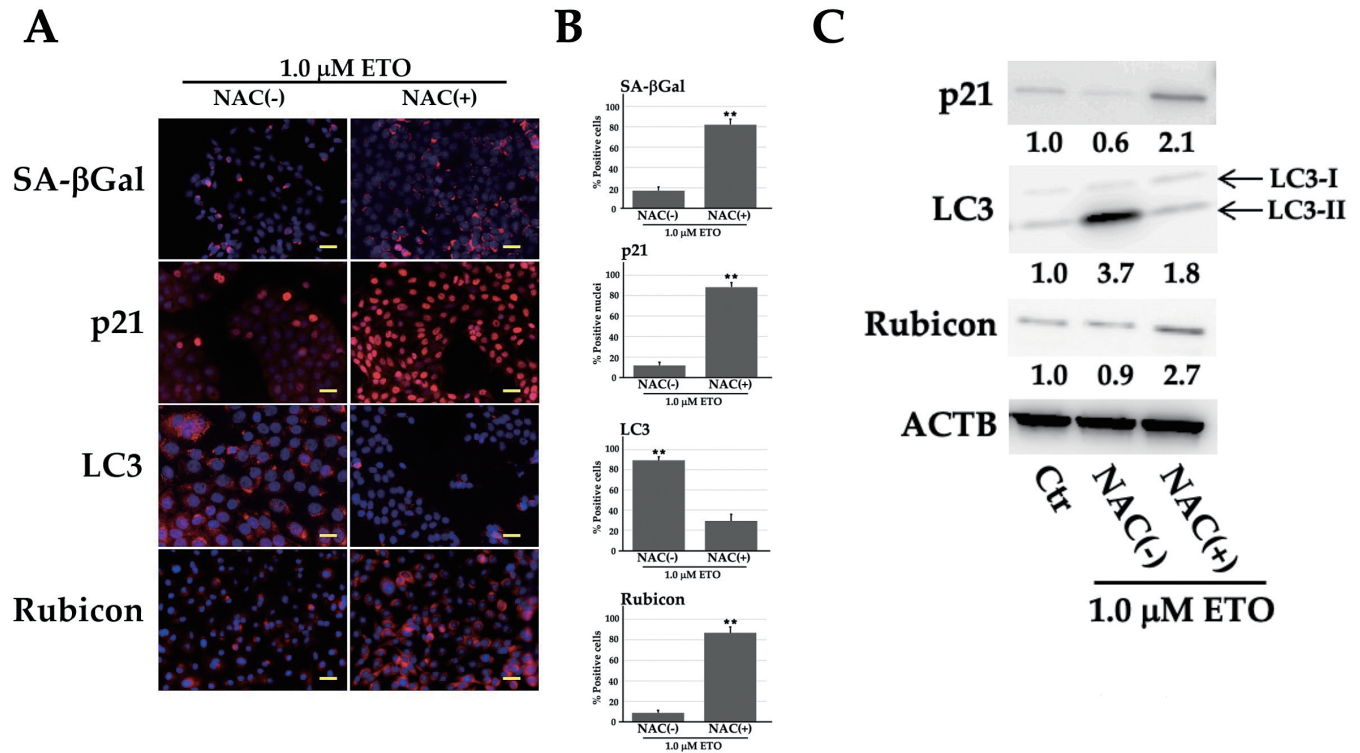

Figure 5. Autophagy inhibition enhances DNA damage response-related cellular senescence. (A) Immunofluorescence images of SA-β-Gal, p21, LC3, and Rubicon staining (red) in 1.0-μM ETO-treated cells with or without NAC pretreatment. Nuclei were counterstained with Hoechst 33342 (blue). Scale bars represent 20 μm. (B) Semiquantification of the percentage of positive cells or nuclei that were stained with SA-β-Gal, p21, LC3, and Rubicon using WinROOF image analysis software. Data represent the mean ± SD of three independent experiments. n.s., not significant. ** *P* < 0.01. (C) Western blot analysis of SA-β-Gal, p21, LC3, Rubicon, and ACTB. NAC, N-acetylcysteine; NAC (−), cells pretreated without NAC; NAC (+), cells pretreated with NAC; ETO, etoposide; ACTB, β-actin.

regulators of autophagy in HaCaT cells treated or untreated with ETO. We first examined the expression of LC3 and Beclin-1 through immunocytochemical and WB analyses. The conversion of LC3-I to autophagosome-associated LC3-II was revealed in autophagy-activated cells[11, 30]. Through immunocytochemical approaches, several LC3-II-positive autophagosomes were observed in 1.0-μM ETO-treated cells (91.5% ± 5.8%) as compared to the control (3.2% ± 1.9%; $p < 0.01$) and 5.0-μM ETO-treated cells (33.3% ± 11.6%; $p < 0.01$) (Fig. 4A, B). An increased percentage of LC3-positive cells correlated with that of Beclin-1 in 1.0-μM ETO-treated cells (Fig. 4A, B). WB analysis showed increased expression levels of both LC3-II and Beclin-1 in 1.0-μM ETO-treated cells as compared with the control and 5.0-μM ETO-treated cells (Fig. 4C). In contrast to LC3 and Beclin-1 expression, cytoplasmic staining with Rubicon was predominant in 5.0-μM ETO-treated cells (Fig. 4A). Additionally, 5.0-μM ETO-treated cells (91.1% ± 3.5%) had a greater percentage of Rubicon-positive cells than controls (4.3% ± 3.0%; $p < 0.01$) and 1.0-μM ETO-treated cells (10.9% ± 1.6%; $p < 0.01$) (Fig. 4B). WB analysis revealed that the expression levels of Rubicon were remarkably higher in 5.0-μM ETO-treated cells than in controls and in 1.0-μM ETO-treated cells (Fig. 4C). Our results indicate that DDR-related senescent cells treated with 5.0 μM of ETO showed increased expression of Rubicon but not LC3-II and Beclin-1. These findings suggest that induction of DDR-related senescence may suppress autophagy.

Autophagy suppression enhances DDR-related cellular senescence

To elucidate the role of autophagy in the induction of senescence, we examined whether inhibition of autophagy by NAC can induce cellular senescence in 1.0-μM ETO-treated cells. After pretreatment with NAC, the percentages of both SA-β-Gal- (82.0% ± 5.3%) and p21-positive (88.3% ± 4.3%) cells increased in 1.0-μM ETO-treated cells [NAC (+)] as compared with cells without NAC pretreatment [NAC (−)] (SA-β-Gal, 17.4% ± 3.7%; $p < 0.01$: p21, 12.0% ± 3.1%; $p < 0.01$) (Fig. 5A, B). Results of the WB analysis of expression levels of p21 supported the immunocytochemical findings (Fig. 5C). For autophagy regulators, NAC pretreatment decreased the number of LC3-II-positive autophagosomes in NAC (−) cells (89.5% ± 3.5% vs. NAC (+) 29.3% ± 6.5%; $p < 0.01$] (Fig. 5A, B). Meanwhile, the WB results showed upregulated expression levels of LC3-II in NAC (−) cells as compared with NAC (+) cells (Fig. 5C). Additionally, Rubicon expression was upregulated in NAC (+) cells (Fig. 5A–C). The percentage of Rubicon-positive cells was significantly higher in NAC (+) cells (86.9% ± 5.4%) than in NAC (−) cells (9.0% ± 2.4%; $p < 0.01$) (Fig. 5B). WB analysis revealed that the expression levels of Rubicon were enhanced in NAC (+) cells as compared with NAC (−) cells. These findings suggest that autophagy suppression due to increased Rubicon expression may induce DDR-related senescence.

Discussion

It was reported that autophagy can regulate cellular senescence[13-15, 31, 32]. This study provided three lines of supportive evidence concerning the effects of autophagy on the induction of DDR-related cellular senescence in ETO-treated HaCaT cells. First, ETO treatment induces DDR-related cellular senescence via the activation of the ATM signaling pathway. Second, induction of DDR-related cellular senescence attenuates autophagy in association with the upregulation of Rubicon expression. Third, suppression of autophagy by NAC can accelerate cellular senescence.

The present study revealed that ETO treatment induces DDR-related

cellular senescence in HaCaT cells. ETO acts on topoisomerase II, which is an enzyme involved in adduction within the double helix, resulting in DSBs and DNA damage[27]. The Pap staining results imply that chromatin alteration, which is a morphological feature of DNA damage[25, 33, 34], is caused by ETO treatment. Nuclear chromatin clumping was more frequent in 5.0-μM ETO-treated cells than in 1.0-μM ETO-treated cells and may reflect DSB-leading genomic instabilities in ETO-treated cells. The genomic instabilities in the treated cells were represented by the increased number of nuclear foci stained with both γH2AX and 53BP1. In the DDR pathway, histone H2AX receives a phosphorylation switch from Tyr142 (H2AX-pY142) to pSer139 (γH2AX)[35, 36]. γH2AX is the first step in recruiting and localizing DNA repair proteins. 53BP1, which is a protein that was proposed to function as a transcriptional coactivator of the p53 tumor suppressor, is activated early in DDR to repair DSBs[37]. As nuclear foci stained with both γH2AX and 53BP1 localized at sites of DSBs[37], this showed that DNA damage was more severe in 5.0-μM ETO-treated cells than in 1.0-μM ETO-treated cells, suggesting that 1.0 μM of ETO induces only mild DDR, resulting in less nuclear chromatin clumping. In this study, an increased percentage of SA-β-Gal-positive cells was observed in 5.0-μM ETO-treated cells as compared with 1.0-μM ETO-treated cells. The most widely used biomarker for senescent and aging cells is SA-β-Gal, which is an abundant lysosomal enzyme with an optimal pH of 4 in young or immortal cells; enzyme activity is activated at a pH of 6 in senescent cells. Therefore, SA-β-Gal expression is highly correlated with cellular senescence in cultured cells[7, 8]. These findings suggest that 5.0-μM ETO-induced DDR may subsequently induce cellular senescence in HaCaT cells.

In this study, enhanced expression of pATM, pp53, and p21 was observed in senescent cells treated with 5.0 μM ETO, indicating that the activated ATM pathway contributed to DDR-related senescence. ATM, which is known as a stress sensor, was identified as a central player in the DDR pathway[38]. ATM bound to DSBs undergoes autophosphorylation and activation into pATM, which facilitates the p53/p21 axis by phosphorylating both p53 and its ubiquitin ligase Murine double minute 2, leading to the stabilization of p53 levels[39]. Studies reported that activated ATM can finely tune the balance between senescence and apoptosis[29, 40]. Upon cellular stimulation, p53 regulates the expression of target genes involved in cell cycle arrest, DNA repair, senescence, and apoptosis[41] and plays a critical role in the maintenance of genomic integrity through its role in DDR[42]. Loss of p53 function directly and indirectly promotes chromosomal instability, including induction of senescence or apoptosis of cells[43]. After induction of DDR and following activation of p53 (pp53) by pATM, expression of p21, which is a pleiotropic inhibitor of cyclin/cyclin-dependent kinase complex that mediates cell cycle progression, is upregulated[44]. One of the most widely studied pathways involved in the regulation of cellular senescence is the p53/p21 pathway[45, 46]. In our study, senescent cells induced by treatment with 5.0 μM of ETO showed upregulated expression of both pp53 and p21, indicating transcriptional activation of p21 via pATM and pp53. These findings suggest that induction and initiation of DDR-related cellular senescence may be mediated by the activated ATM/p53/p21 signaling pathway.

Although senescence and autophagy play important roles in homeostasis, interrelation between both processes is considered a double-edged sword. Several studies suggest that autophagy promotes senescence, whereas other reports showed that autophagy prevents senescence[4, 16-18, 20]. In this study, we revealed that expression of both LC3 and Beclin-1 were decreased in DDR-related senescent cells. These results provide evidence that induction and initiation of DDR-related cellular senes-

cence suppresses autophagy and is supported by the increased expression of Rubicon, which is a negative regulator of autophagy, in 5.0-μM ETO-treated senescent cells. In autophagy, class III phosphatidylinositol-3-kinase (PI3KC3), which consists of three core components (Vps34, p150, Beclin-1), plays an important role in autophagosome biogenesis by catalyzing the formation of phosphatidylinositol-3-phosphate[47]. Rubicon directly binds with PI3KC3-related components and suppresses their function, resulting in inhibition of autophagosome–lysosome fusion processes[48]. However, overexpression of Rubicon leads to autophagy impairment in senescent cells. In contrast, 1.0-μM ETO-treated nonsenescent cells showed neither downregulated expression of LC3 and Beclin-1 nor increased expression of Rubicon. These findings suggest that Rubicon-regulated autophagy impairment may be required for the induction and initiation of DDR-related cellular senescence depending on the degree and/or severity of DDR.

Pharmacological inhibition of autophagy accelerates DDR-related cellular senescence in 1.0-μM ETO-treated cells, which showed less expression of senescent markers. NAC pretreatment led to increased expression of both SA-β-Gal and p21 in addition to decreased expression of positive regulators of autophagy (LC3 and Beclin-1). Increased expression of Rubicon was also observed in NAC (+) 1.0-μM ETO-treated cells. These results suggest that autophagy may inhibit induction of DDR-related cellular senescence in ETO-treated cells with mild DDR, and that autophagic protection from cellular senescence may be regulated by Rubicon expression. This speculation supports the results of recent studies indicating that impaired autophagy via Rubicon overexpression enhanced cellular senescence[19, 20]. Together, our findings suggest that autophagy may be protective against DDR-related cellular senescence.

We should acknowledge possible limitations to this study, especially the lack of direct evidence of how Rubicon expression is increased to suppress autophagy. Although recent studies showed that Rubicon levels were at least altered by several lifespan-extending conditions in worm and mouse tissues, mechanisms that increase Rubicon levels during senescence remain unclear. This paper also lacks evidence of how Rubicon-induced autophagy impairment enhances activation of the ATM/p53/p21 signaling pathway, although studies reported a connection between DDR and autophagy[28, 49, 50]. Further studies are warranted to examine the roles of autophagy in association with Rubicon in the induction and initiation of DDR-related cellular senescence.

In conclusion, this study revealed that autophagy mediates ETO-induced DDR-related cellular senescence through the activation of the ATM/p53/p21 signaling pathway. Induction of DDR-related cellular senescence is enhanced by autophagy impairment in association with Rubicon overexpression.

Conflict of Interest

The authors declare no conflict of interest.

References

1. Serrano M and Blasco MA. Putting the stress on senescence. Curr Opin Cell Biol 13: 748-753, 2001

2. Roninson I B. Tumor cell senescence in cancer treatment. Cancer Res 63: 2705-2715, 2003

3. Alexander K and Hinds PW. Requirement for p27(KIP1) in retinoblastoma protein-mediated senescence. Mol Cell Biol 21: 3616-3631, 2001

4. Bader AS, Hawley BR, Wilcznska A and Bushell M. The roles of RNA in DNA double-strand break repair. Br J Cancer 122: 613-623, 2020

5. Herranz N and Gil J. Mechanisms and functions of cellular senescence. J Clin Invest 128: 1238-1246, 2018

6. Munoz-Espin D and Serrano M. Cellular senescence: From physiology to pathology. Nat Rev Mol Cell Biol 15: 482-496, 2014

7. Lee BY, Han JA, Im S, Morrone A, Johung K, Goodwin EC, Kleijer WJ, DiMaio D and Hwang ES. Senescence-associated beta-galactosidase is lysosomal beta-galactosidase. Aging Cell 5: 187-195, 2006

8. Kurz DJ, Decary S, Jong Y and Erusalimsky JD. Senescence-associated (beta)-galactosidase reflects an increase in lysosomal mass during replicative ageing of human endothelial cells. J Cell Sci 113: 3613-3622, 2000

9. Narita M, Nunez S, Heard E, Narita M, Lin AW, Hearn SA, Spector DL, Hannon GJ and Lowe SW. Rb-mediated heterochromatin formation and silencing of E2F target genes during cellular senescence. Cell 113: 703-716, 2003

10. Zhang R, Poustovoitov MS, Ye X, Santos HA, Chen W, Daganzo SM, Erzberger JP, Serebriiskii IG, Canutescu AA, Dunbrack RL, Pehrson JR, Berger JM, Kaufman PD and Adams PD. Formation of MacroH2A-containing senescence-associated heterochromatin foci and senescence driven by ASF1a and HIRA. Dev Cell 8: 19-30, 2005

11. Mizushima N, Levine B, Cuervo AM and Klinonsky DJ. Autophagy fights disease through cellular self-digestion. Nature 451: 1069-1075, 2008

12. Cuervo AM, Bergamini E, Brunk UT, Droge W, Ffrench M and Terman A. Autophagy and aging: The importance of maintaining "clean" cells. Autophagy 1: 131-140, 2005

13. Rajendran P, Akzagrabu AM, Hanieh H, Kumar SA, Ammar RB, Rengarajan T and Alhoot MA. Autophagy and senescence: A new insight in selected human diseases. J Cell Physiol 234: 21485-21492, 2019

14. Kwon Y, Kim JW, Jeoung JA, Kim MS and Kang C. Autophagy is pro-senescence when seen in close-up, but anti-senescence in long-shot. Mol Cells 40: 607-612, 2017

15. Gewirtz DA. Autophagy and senescence: A partnership in search of definition. Autophagy 9: 808-812, 2013

16. Yamaguchi M, Kajiya H, Egashira R, Yasunaga M, Hagio-Izaki K, Sato A, Toshimitsu T, Naito T and Ohno J. Oxidative stress-induced interaction between autophagy and cellular senescence in human keratinocytes. J Hard Tissue Biol 27: 199-208, 2018

17. Luo Y, Zou P, Zou J, Wang J, Zhou D and Liu L. Autophagy regulates ROS-induced cellular senescence via p21 in a p38 MAPKalpha dependent manner. Exp Gerontol 46: 860-867, 2011

18. White E and Lowe SW. Eating to exit: Autophagy-enabled senescence revealed. Genes Dev 23: 784-778, 2009

19. Nakamura S, Oba M, Suzuki M, Takahashi A, Yamamuro T, Fujiwara M, Ikenaka K, Minami S, Tabata N, Yamamoto K, Kubo S, Tokumura A, Akamatsu K, Miyazaki Y, Kawabata T, Hamasaki M, Fukui K, Sango K, Watanabe Y, Takabatake Y, Kitajima TS, Okada Y, Mochizuki H, Ksaka Y, Antebi A and Yoshsimori T. Suppression of autophagic activity by Rubicon is a signature of aging. Nat Commun 10: 847, 2019

20. Yamamoto-Imoto H, Minami S, Shioda T, Yamashita Y, Sakai S,

Maeda S, Yamamoto T, Oki S, Takashima M, Yamamuro T, Yanagawa K, Edahiro R, Iwatani M, So M, Tokumura A, Abe T, Imamura R, Nonomura N, Okada Y, Ayer DE, Ogawa H, Hara E, Takabatake Y, Isaka Y, Nakamura S and Yoshimori T. Age-associated decline of MondoA drives cellular senescence through impaired autophagy and mitochondrial homeostasis. Cell Rep 38: 110444, 2022

21. Xie BS, Zhao HC, Yao SK, Zhuo DX, Jin B, LV DC, Wu CL, Ma DL, Gao C, Shu XM and Ai ZL. Autophagy inhibition enhances etoposide-induced cell death in human hepatoma G2 cells. Int J Mol Med 27: 599-606, 2011

22. Teng YN, Chang HC, Chao YY, CHeng HL, Lien WC and Wang CY. Etoposide triggers cellular senescence by inducing multiple centrosomes and primary cilia in adrenocortical tumor cells. Cells 10: 1466, 2021

23. Lin X, Wei M, Song F, Xue DI and Wang Yet. N-acetylcysteine (NAC) attenuating apoptosis and autophagy in RAW264.7 cells in response to incubation with mycolic acid from bovine mycobacterium tuberculosis complex. Pol J Microbiol 69: 223-229, 2020

24. Wang C, Chen K, Xia Y, Dai W, Wang F, Shen M, Cheng P, Wang J, Lu J, Zhang Y, Yang J, Zhu R, Zhang H, Li J, Zheng Y, Zhou Y and Guo G. N-acetylcysteine attenuates ischemia-reperfusion-induced apoptosis and autophagy in mouse liver via regulation of the ROS/JNK/Bcl-2 pathway. PLoS One 9: e108855, 2014

25. Dos Santos A, Cook AW, Gough RE, Schilling M, Olszok NA, Brown I, Wang L, Aaron J, Martin-Fernandez ML, Rehfeldt F and Toseland CP. DNA damage alters nuclear mechanics through chromatin reorganization. Nucleic Acids Res 49: 340-353, 2021

26. Tamamori-Adachi M, Koga A, Susa T, Fujii H, Tsuchiya M, Okinaga H, Hisaki H, Iizuka M, Kitajima S and Okazaki T. DNA damage response induced by etoposide promotes steroidogenesis via GADD45A in cultured adrenal cells. Sci Rep 8: 9636, 2018

27. Bang M, Kim DG, Gonzales EL, Kwon KH and Shin CY. Etoposide induces mitochondrial dysfunction and cellular senescence in primary cultured rat astrocytes. Biomol Ther 27: 530-539, 2019

28. Guo C and Zhao Y. Autophagy and DNA damage repair. Genome Inst Dis 2020. doi: 10.1007/s42764-020-00016-9

29. Stagni V, Ferri A, Cirotti C and Darila D. ATM kinase-dependent regulation of autophagy: A key player in senescence? Front Cell Dev Biol 8: 599048, 2020

30. Mizushima N and Levine B. Autophagy in mammalian development and differentiation. Nat Cell Biol 12: 823-830, 2010

31. Cayo A, Segovia R, Venturini W, Moore-Carrasco R, Valenzuela C and Brown N. mTOR activity and autophagy in senescent cells, a complex partnership. Int J Mol Sci 22: 8149, 2021

32. Rastaldo R, Vitale E and Giachino C. Dual role of autophagy in regulation of mesenchymal stem cell senescence. Front Cell Dev Biol 8: 276, 2020

33. Komagata H, Ichimura T, Matsuta Y, Ishikawa K, Shinoda N, Kobayashi N and Sasaki A. Feature analysis of cell nuclear chromatin distribution in support of cervical cytology. J Med Imaging 4: 047501, 2017

34. Kumar R, Horikoshi N, Singh M, Gupta A, Misra HS, Albuquerque K, Hunt CR and Pandita TK. Chromatin modifications and the DNA damage response to ionizing radiation. Front Oncol 2: 214, 2012

35. Lukas J, Lukas C and Bartek J. More than just a focus: The chromatin response to DNA damage and its role in genome integrity maintenance. Nat Cell Biol 13: 1161-1169, 2011

36. Rossetto D, Truman AW, Kron SJ and Cote J. Epigenetic modifications in double-strand break DNA damage signaling and repair. Clin Cancer Res 16: 4543-4552, 2010

37. Schultz LB, Chehab NH, Malikzay A and Halazonetis TD. p53 binding protein 1 (53BP1) is an early participant in the cellular response to DNA double-strand breaks. J Cell Bio 151: 1381-1390, 2000

38. Shiloh Y and Ziv Y. The ATM protein kinase: regulating the cellular response to genotoxic stress, and more. Nat Rev Mol Cell Biol 14: 197-210, 2013

39. HuW, Feng Z and Levine AJ. The regulation of multiple p53 stress responses is mediated through MDM2. Genes Cancer 3: 199-208, 2012

40. Mijit M, Caracciolo V, Melillo A, Amicarelli F and Giordao A. Role of p53 in the regulation of cellular senescence. Biomolecules 10: 420, 2020

41. Fischer M. Census and evaluation of p53 target genes. Oncogene 36: 3943-3956, 2017

42. Williams AB and Schumacher B. p53 in the DNA-damage-repair process. Cold Spring Harb Perspect Med 6: a026070, 2016

43. He Q, Au B, Kulkarni M, Shen Y, Lim KJ, Kaimaiti J, Wong CK, Luijten MNH, Chong HC, Lim EH, Rancati G, Sinha I, Ru Z, Wang X, Connolly JE and Crasta KC. Chromosomal instability-induced senescence potentiates cell non-autonomous tumourigenic effects. Oncogenesis 7: 62, 2018

44. Dotto GP. p21(WAF1/Cip1): More than a break to the cell cycle? Biochim Biophys Acta 1471: M43-56, 2000

45. Malaquin N, Carrier-Leclerc A, Dessureault M and Rodier F. DDR-mediated crosstalk between DNA-damaged cells and their microenvironment. Front Genet 6: 94, 2015

46. Vasileiou PVS, Evangelou K, Vlasis K, Fildisis G, Panayiotidis MI, Chronopoulos E, Passias PG, Kouloukoussa M, Gorgoulis VG and Havaki S. Mitochondrial homeostasis and cellular senescence. Cells 8: 686, 2019

47. Simonsen A and Tooze SA. Coordination of membrane events during autophagy by multiple class III PI3-kinase complexes. J Cell Biol 186: 773-782, 2009

48. Minami S, Nakamura S and Yoshimori T. Rubicon in metabolic diseases and ageing. Front Cell Dev Biol 9: 816829, 2021

49. Czarny P, Pawlowska E, Bialkowska-Warzecha J, Kaarniranta K and Blasiak J. Autophagy in DNA damage response. Int J Mol Sci 16: 2641-2662, 2015

50. Liang, N., He Q, Liu X and Sun He. Multifaceted roles of ATM in autophagy: From nonselective autophagy to selective autophagy. Cell Biochem Funct 37: 177-184, 2019